A Comparative Study on the Seismic Performance of Concrete and Steel Diagrid Structures

by

Mingze Sun

B.S. Civil Engineering
Cornell University, 2014

SUBMITTED TO THE DEPARTMENT OF CIVIL AND ENVIRONMENTAL ENGINEERING IN PARTIAL FULFILLMENT OF THE REQUIREMENTS FOR THE DEGREE OF
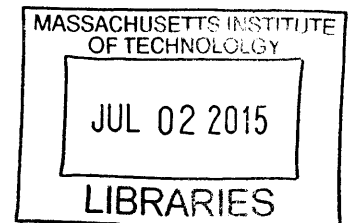
MASTER OF ENGINEERING IN CIVIL AND ENVIRONMENTAL ENGINEERING
AT THE
MASSACHUSETTS INSTITUTE OF TECHNOLOGY

JUNE 2015

Signature of Author: **Signature redacted**

Department of Civil and Environmental Engineering
May 20, 2015

Certified by: **Signature redacted**

Jerome J. Connor
Professor of Civil and Environmental Engineering
Thesis Supervisor

Accepted by: **Signature redacted**

Heidi M. Nepf
Donald and Martha Harleman Professor of Civil and Environmental Engineering
Chairman, Departmental Committee for Graduate Students

A Comparative Study on the Seismic Performance of Concrete and Steel Diagrid Structures

by

Mingze Sun

Submitted to the Department of Civil and Environmental Engineering
on May 20, 2015 in Partial Fulfillment of the
Requirements for the Degree of Master of Engineering in
Civil and Environmental Engineering

ABSTRACT

In recent years, concrete Diagrids have been more widely used in the current Diagrid building designs, especially with mid-rise buildings. Looking through the entire portfolio of completed Diagrid structures, there are very few Diagrid tall building structures located in the area where seismic forces govern the lateral design. An investigation on the seismic performance of concrete Diagrid structures would give the engineers a better understanding of this unique type of structural system.

A comparative research was conducted in this paper on the seismic performance of concrete Diagrid structures comparing to steel Diagrid structures. Two building height scenarios were considered for mid-rise 8-story buildings and high-rise 60-story buildings. Response spectrum analysis was used for two different earthquake locations corresponding to code based seismic design approach using ASCE 7-10. The seismic performances of both types of Diagrid structures were also compared to 8-story moment frame buildings and 60-story outrigger buildings for the two scenarios respectively.

With all member sizes set to be fixed across all models, steel Diagrids were found to be performing better than concrete Diagrids in terms of natural period and controlling top drifts while concrete was tested to be better at controlling top accelerations. Comparing to outrigger and moment frame systems, both concrete and steel Diagrid structures were tested to be stiffer and more effective in restraining top drifts but less satisfying in limiting top accelerations.

Thesis Supervisor: Jerome Connor
Title: Professor of Civil and Environmental Engineering

Acknowledgements

I would like to thank my parents and friends for their love and trust all these years. Without their support and guidance, I would not be able to do what I want and I could not have achieved all these great things in life.

I would like to thank Professor Jerome Connor for his help and support in writing this thesis. I would also like to thank Dr. Pierre Ghisbain for all his patience and kindness in answering all the questions I encountered. I would like to thank Professor John Ochsendorf for his career and life guidance throughout the year.

I would like to thank all my awesome MEng classmates. You are the most amazing group of students I have ever met and I am honored to have worked with you. I would like to thank Jianhua Jiang, Han Wu and Zifan Yang for the brotherhood and wish you all achieve great success in the future.

Finally, and most importantly, I would like to thank Xiaoxiao for her love and company during my life at MIT.

Contents

List of Figures

List of Tables

Chapter 1 Introduction

Diagrid structures are becoming increasingly attractive and favorable to engineers and architects because of their structural efficiency and visual elegance. In recent years, Diagrid structures have been emerging significantly all around the world since Sir Norman Foster's completing the notable Swiss Re Building in London and Hearst Tower in New York City. The use of perimeter diagonal members enables the building structure to sustain both gravity and lateral loads through axial forces instead of bending, eliminating vertical columns on the exterior. While most of current Diagrid structures are made out of steel, concrete grids are also used in the diagonal member design in the form of pre-stressed concrete or more often composite steel/concrete sections such as concrete filled steel tubes.

However, little research has been conducted in the aspect of investigating the seismic behavior and dynamic response of concrete Diagrid structures. Looking through the entire portfolio of completed Diagrid structures, there are very few Diagrid tall building structures located in the area where seismic forces govern the lateral design. For a Diagrid structure under the event of an earthquake, ductile yielding of diagonal members which also carry substantial vertical gravity loads is problematic, since it's hard to have inelastic yielding of the diagonal bracing members for the seismic forces while still sustaining the gravity loads and avoiding instability.

The purpose of this paper is to investigate the seismic behavior and dynamic response of Diagrid structures using concrete, with comparison to pure steel Diagrid structures and other structural systems. First of all, an introduction and overview of Diagrid structural system will be presented. Code Based Seismic Design approach will then be introduced and explained and a literature review of completed researches on seismic performance of Diagrids will be included. Diagrid structural models with varying design parameters will then be taken into analysis, focusing on the seismic behavior comparison for different Diagrid materials. Two different aspect ratios, one for eight-story mid-rise building and the other for sixty-story high-rise building, will be considered in the investigation of Diagrid structures. Different building locations and seismic inputs will be taken into consideration for the structural analysis. In order to have a more thorough understanding of the differences, the comparison study will also include other popular structural systems for the two building heights. For the eight-story mid-rise building, a comparison study will be performed on concrete Diagrids, steel Diagrids and traditional moment frame buildings. As

for a typical high-rise building of sixty stories, a similar analysis will be conducted comparing with outrigger system, which is the prevalent structural system used in contemporary high-rise designs.

Chapter 2 Diagrid Structural System

2.1 Overview of Diagrid System

As an increasingly popular structural feature in current building designs, "Diagrid" is well defined as a blending of "diagonal" and "grid" to represent the uniform and distributed triangulated configuration (Boake, 2013). Diagrid system is recognized as a unique structural system as their perimeter diagonal members provide stiffness for both lateral and gravity loadings, which is much more efficient than a conventional bracing system where the braces only provide lateral stiffness. The simple load diagram of a Diagrid structure is shown in Figure 1 (Singh et al, 2014). The stiffness of the Diagrid depends on the axial stiffness and strength of the diagonal members. More specifically, if setting the cross-section, length and material property as constants, the main variable for Diagrid stiffness is the diagonal angle. As the angle varies, Diagrids' lateral and vertical stiffness would change accordingly. As the diagonal members are designed to be more vertical (i.e. the sine of the diagonal angle increases), the gravity stiffness would increase while the lateral stiffness would decrease and vice versa (Liptack, 2013).
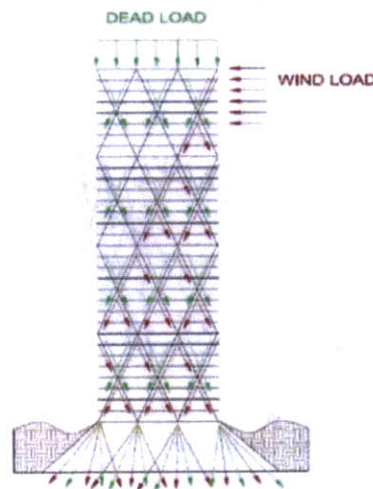
Figure 1 Simplified Load Diagram for Typical Diagrid Structure (Singh et al.)

The implementation of this unique geometry configuration has helped eliminating most of the conventional columns and structural cores for low-rise buildings, enabling a great clear span for architectural innovation and aesthetic elegance. For high-rise buildings over 50 stories, a structural core is generally incorporated into the structural design with the perimeter Diagrid system, providing primarily

gravity supports and also some lateral stiffness to the structure. In this structural core plus perimeter Diagrids combination system, the core provides about 20 percent of the total lateral stiffness while the Diagrids take the majority of lateral loads (Moon et al., 2005).

The structural efficiency of the Diagrid system not only stands out in terms of eliminating vertical columns for material savings, but more importantly, transforming loads through axial forces instead of relying on the bending rigidity of traditional columns. A typical Diagrid module under lateral loadings is shown in Figure 2. Comparing to traditional moment frame structures which carry shear through bending, Diagrid system is much more efficient in the aspect of reducing shear deformations due to its axial action of diagonal members. For high-rise buildings over 50 stories, Diagrid structures also stand out in their structural efficiency in terms of structural core design. One of the most popular structural systems nowadays for skyscrapers is outrigger system with either steel braced cores or reinforced concrete cores. The utilization of outriggers would significantly reduce the moment and lateral drift but lacking shear rigidity, which needs to be designed into the structural core for the completeness of outrigger system. For Diagrids, the triangulated configuration provides both bending and shear rigidity, leaving the structural core with lower shear rigidity requirements (Moon et al., 2005).
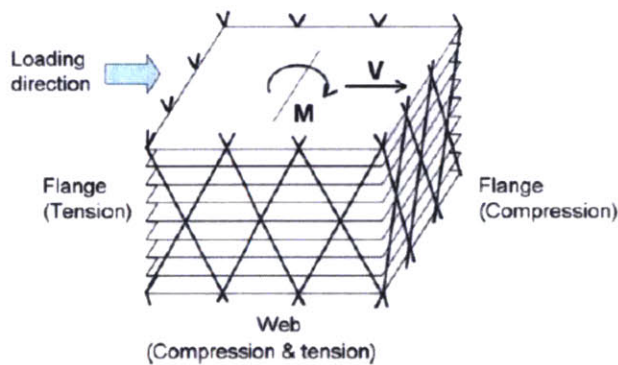
Figure 2 Typical Diagrid module (Moon et al.)

2.2 Materiality

Diagrid structures can be constructed using a variety of different materials, including steel, concrete, timber and composites. However, looking through the list of Diagrid precedent structures, the majority of these are made out of steel. Some of these steel Diagrids are utilizing standard wide flange sections or hollow structural tubes sections (HSS), while some other projects require customized sections for architectural purposes, as shown in Figure 3. The predominant use of steel in diagonal member designs is a result of easier fabrication of joints and faster construction sequence comparing to other materials.

(a) Steel HSS Node   (b) Steel Customized Plate Node

Figure 3 Steel Diagrid Nodes using HSS Sections and Customized Plate Sections (Boake)

Concrete, being the most significant construction material for modern building structures, does not have a great number of applications in the area of Diagrid designs. The most outstanding reason for such lack of precedents is the simple fact that concrete is bad in tension. As simple statics imply, the triangular geometry of Diagrid structures requires the diagonal members to take both compression and tension forces. The huge tension force created during the process would cause severe problems if using concrete as the main construction material especially for a high-rise building. Another reason for not using concrete is the constructability issue, where connections to nodes would be hard to fabricate and construct on site using cast in place reinforced concrete. The framework being expensive and the construction being slow are also the main disadvantages of a concrete Diagrid structure.

However, in recent years, there is a noticeable tendency for Middle East and East Asian countries to employ the design of composite concrete/steel sections for Diagrids, especially concrete filled steel tubes, as shown in Figure 4. By using this composite section, the issue of tension would be well solved by the outer steel tube while taking advantages of the concrete infill to take major compression forces. From the constructability aspect, the connections could be welded into hub sections connecting the steel tubes together. The application of steel tubes also serves as the framework for concrete pouring, enhancing the feasibility of this composite section. A more detailed overview of this composite section will be presented in the next section 2.3 Concrete Filled Steel Tubes.

An alternative way of dealing with concrete tension is through prestressing the concrete. In order to achieve the prestress state of concrete, pre-tension or post-tension methods could be utilized with tendons. By applying a pre-loading compression force, the concrete could still be in a compressive state when the actual loading is causing tension in the element, reducing the failure due to concrete cracking or even rupturing in tension. However, prestressed concrete Diagrid structures are not often seen in the current building designs. The most important reason is the cost of construction, including framework, prestressing, curing, etc. Also, the connections for prestressed concrete diagonal members are very expensive and hard to fabricate on site at height. All of these issues made prestressed concrete Diagrid structures unfavorable in an owner's point of view, especially for mixed-use high-rise buildings where budgets and profits are the main focuses of the project.
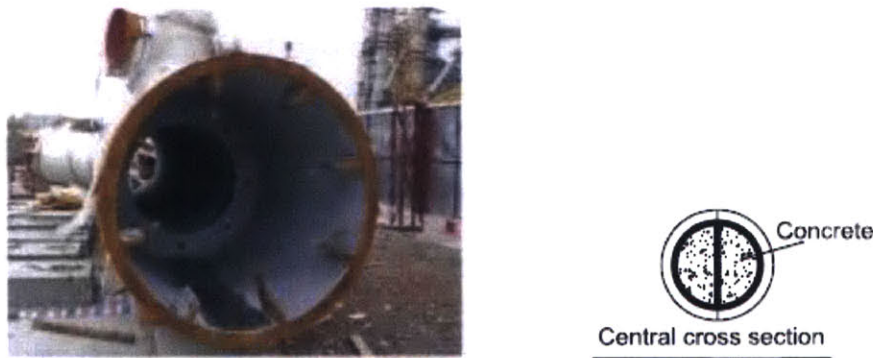
Figure 4 Composite Section of Concrete Filled Steel Tube (Boake)

2.3 Concrete Filled Steel Tubes

Concrete has been the most widely used construction material in the current building design. When it is used with steel to form a composite section, concrete can be either poured to surround the steel or poured inside the HSS steel tube section. Both of these two methods function as structural reinforcement of the building as well as providing fire resistance to pure steel systems.

The application of concrete filled steel tube is mostly in column designs of building structures, providing mainly lateral stiffness in either braced or unbraced systems. For Diagrid designs in the past decade, an increasing amount of composite Diagrid structures have employed the use of concrete filled steel tubes for the design of diagonal members, especially for high-rise buildings in Middle East and Asian countries where concrete is more often the regional construction material and labor cost is relatively low.

The benefits of concrete filled steel tube sections are summarized below according to Huang et al. on the properties of concrete filled steel tubes (2010):

- The composite cross section improves the tensile strength comparing to pure reinforced concrete section as the perimeter steel provides tension resistance.
- Perimeter steel also enhances the stiffness of the composite section as the steel, with greater modulus of elasticity than concrete, locates farthest from the centroid to maximize the moment of inertia.
- The infilled concrete provides the required compressive strength with the confinement of the exterior steel; more importantly, the concrete section delays and sometimes prevents the steel from local buckling.
- The steel tube also prevents concrete from spalling and concrete creeps are often smaller comparing to normal reinforced concrete section.
- The existence of perimeter steel eliminates the need of additional framework and reinforcing bars; concrete can then be infilled through pump-up method. This feature dramatically improves the constructability of Diagrids and saves both labor and cost.
- Concrete helps improve the fire resistance of the cross section comparing to pure steel section.

Concrete filled steel tubes are becoming popular as the combination of the two materials have some major advantages over pure steel sections or pure reinforced concrete sections in the structural aspect of

Diagrid designs. These advantages are more outstanding when this cross section is being applied to a high-rise building scenario with large diagonal members.

However, the Diagrids' connection design and fabrication process is still one of the most challenging issues to consider with the use of concrete filled steel tube sections. Most of such connection welding could not be pre-fabricated and has to be done on site, which would cause potential delays in project construction schedule or safety concerns of construction workers when performing work at height.

2.4 Diagrid System's Evolving Process

Diagrid system is evolving as structural engineers and architects are constantly seeking improvement and innovations towards efficiency, aesthetics and sustainability. Maqhareh conducted a list of case reviews on the current development of Diagrid structures and they are summarized and reorganized in the following (2014).

Even though the current prevalence of Diagrid structures was inspired by Sir Norman Foster's designs of world-famous Swiss Re Tower in London and Hearst Tower in New York City, the earliest appearance of a pure Diagrid system could be dated back to the 1920s by Vladimir Shukhov completing the Shukhov Tower in Moscow, Russia. The tower is 350m high constructed in steel in the form of a hyperbolic grid, giving the structure an unobstructed view of structural skeleton, as shown in Figure 5. The Shukhov Tower achieved great efficiency by minimizing the construction material while providing required stiffness through its Diagrid feature. It was an extremely innovative and efficient design concept back at that time or even in today's tower designs.
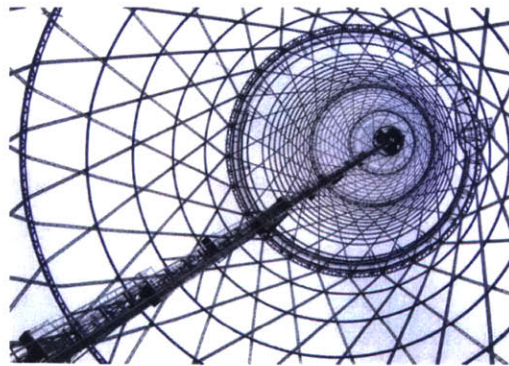
Figure 5 Shukhov Tower in Moscow (commons.wikimedia.org)

In the early stages of Diagrid designs, structural engineers and architects used steel as the dominating material. Designers also fixed diagonal angles throughout the entire building and limited the building heights to below 50 stories. Five of the most notable examples are shown in Figure 6.
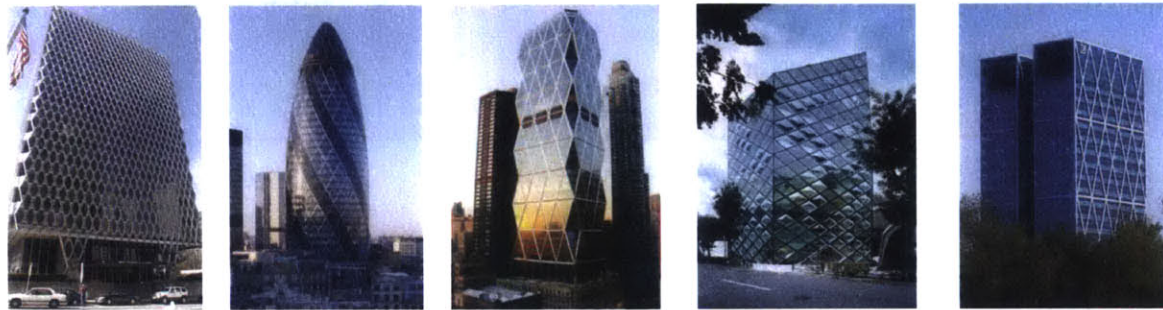
(a) IBM Building   (b) Swiss Re   (c) Hearst Tower   (d) Prada Boutique   (e) Vivaldi Tower

Figure 6 Early Stage Steel Diagrid Structures with Fixed Diagonal Angles under 50 Stories

Within the last ten years, Diagrid structures evolved quite significantly from the early stage designs in a number of different aspects. The most outstanding trend was the use of composite section of concrete filled steel tubes especially in Asian and Middle East countries. Another important progress of designing Diagrid structures was the appearance of high-rise buildings over 50 stories or 200 meters. These high-rise Diagrid structures all became landmarks for each city as their structural elegance elevates to the sky.

From the structural efficiency perspective, an increasing amount of researches have been conducted on the analysis and optimization of Diagrid structural systems. Moon, Connor and Fernandez presented one of the most important researches on the preliminary design of Diagrid structures focusing on the optimal Diagrid angles. The results of this optimization of diagonal angles were then widely taken into consideration for practical Diagrid designs. For example, some Diagrid structures deviated from the traditional uniform and distributed configuration of diagonals and applied a variation of diagonal angles along the vertical span based on varying heights to maximize the structural efficiency of diagonal members. A summary list showing the major milestone Diagrid structures with their Diagrid materials and building heights is presented in Figure 7.
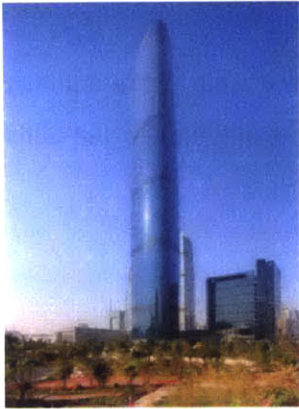
(a) Guangzhou West Tower
Concrete Filled Steel Tube
103 Stories, 440m
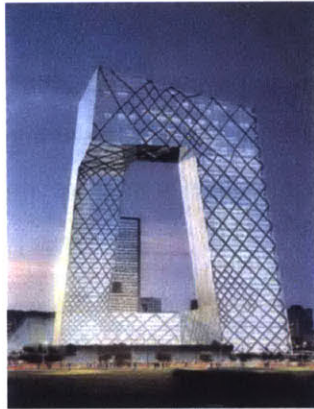
(b) CCTV Tower
Steel Diagrid
44 Stories, 234m
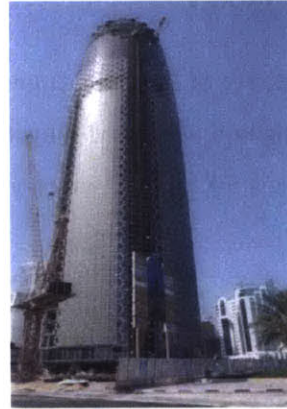
(c) Doha Tower
Reinforced Concrete
45 Stories, 231m

(d) Dorobanti Tower
Concrete Filled Steel Grid
57 Stories, 200m

(e) Lotte Tower
Steel Diagrid
123 Stories, 556m

(f) West Bay Office Tower
Steel & Concrete Diagrid
50 Stories, 230m

Figure 7 Major Milestone Diagrid Structures within the Past Ten Years

Chapter 3 Seismic Design Based on ASCE 7-10

The full title of ASCE 7-10 (ASCE, 2010) is *American Society of Civil Engineers: Minimum Design Loads for Building and Other Structures*. The seismic provisions (page 57-233) consist of a major part of the code. Brief illustrations of the code-based seismic design procedures and requirements for buildings (nonstructural components not included) are summarized.

3.1 Overview of the Seismic Design Process and Analytical Procedures

The process of designing structural systems based ASCE 7-10 could be summarized in three steps:
- Establish design load (Peak Ground Acceleration and/or response spectrum) from corresponding tables (in ASCE 7-10 Chapter 11) and maps (in ASCE 7-10 Chapter 12).
- Perform linear analysis of the structure under design load established in the first step.
    - Three procedures could be used are equivalent lateral force analysis, modal response spectrum analysis and seismic response history procedures.
    - Modification factors (in ASCE 7-10 Chapter 12) are applied in the linear analysis process to determine the required strength of the system to be designed.
- Design the system to have the required strength determined from the second step.

The linear analysis of the structure could be performed through one of the permitted analytical procedures proposed by ASCE 7-10, which are equivalent lateral force analysis, modal response spectrum analysis and seismic response history procedures. The choice of the procedure should be based on different seismic design categories and structural characteristics (Table 12.6-1 in ASCE 7-10). The modal response spectrum analysis and seismic response history procedures are illustrated more in detail in the following two sections.

3.2 Modal Response Spectrum Analysis

The major steps in the modal response spectrum analysis include:
- Determine the number of modes included in the analysis.

- o A sufficient number of modes should be included to obtain a combined modal mass participation of at least 90 percent of the actual mass in each orthogonal horizontal directions considered.
- Compute the member forces for each mode based on the modal properties and response spectra defined based on section 11.4.5 in ASCE 7-10. A typical design response spectrum is shown in Figure 8.
- Divide the obtained member forces by the quantity R/I_e. R is the response modification coefficient as given in Tables 12.2-1, 12.14-1, 15.4-1 or 15,4-2 in ASCE 7-10. I_e is the importance factor prescribed in section 11.5.1 in ASCE 7-10.
- Combine the member forces using the square root of the sum of the squares (SRSS) method or the complete quadratic combination (CQC) method.
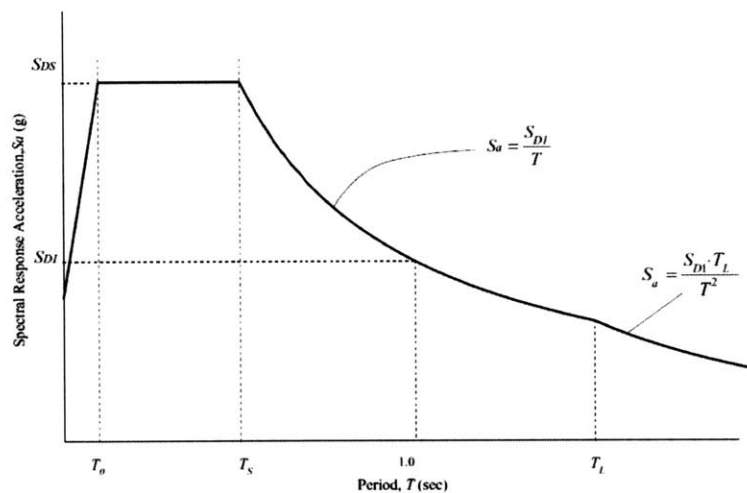
Figure 8 Typical Design Response Spectrum (ASCE7-10)
Note: The key parameters in the spectrum could be decided referring to related instructions
and tables (ASCE 7-10 Chapter 11), and maps (ASCE 7-10 Chapter 12).

3.3 Seismic Response History Procedures

There are two kinds of seismic response history procedures: linear response history procedure and nonlinear response history procedure. In this section, only the linear procedure is introduced here.

A linear response history analysis is an analyzing process that determines the responses of a linear structural model through methods of numerical integration based a suite of (at least three) appropriate ground motions. It should be noted that the ground motions used are scaled from the original earthquake records to be compatible with the design response spectrum for the site.

A typical process of performing a linear time history analysis in a finite element software is:
- Import earthquake records as load curves.
- Calculate the scaling factor and scale the load curves to be compatible with the design response spectrum for a specific site category.
- Specify the damping ratio.
- Set up the output time step and run the analysis.

Chapter 4 Seismic Performance of Diagrid Structures

While a number of researchers focused on studying the optimization and wind response of Diagrid structures, only a few have investigated the seismic behavior of Diagrid system. These completed studies focused solely on steel Diagrid systems. A literature review of previous researches in this area is presented in the following.

4.1 Seismic Performance Factors Determination by SOM

Leading by Bill Baker, Skidmore, Owings & Merrill LLP (SOM) published a paper on determining the seismic performance factors for steel Diagrid structures. They focused on investigating the lack of accuracy on the seismic design parameters for Diagrid system. The two key seismic performance factors they determined were Response Modification Coefficient (R) and Overstrength Factor (Ω_0), whose definitions are shown in Figure 9 according to FEMA 450.
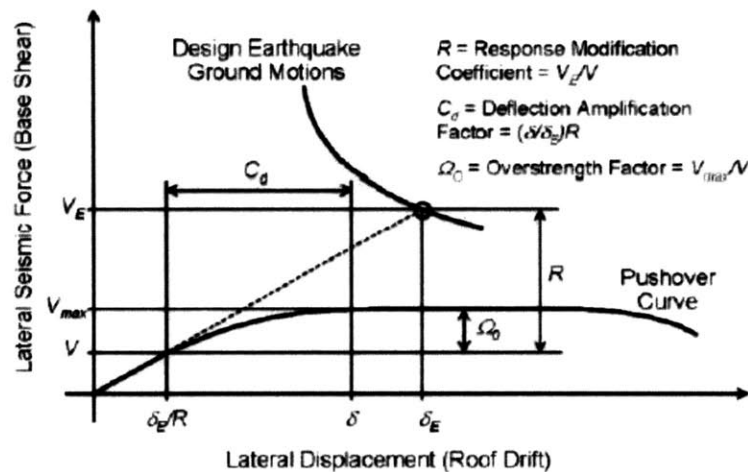
Figure 9 Definition of R and Ω_0 (FEMA 450)

Baker et al. determined the R factor to be 3.64 through an iterative nonlinear static analysis based on FEMA 450 procedures. They conducted the analysis based on a total number of 300 archetype models with varying aspect ratios, diagonal angles, seismic design categories and gravity load intensities. Then they determined Ω_0 to be 1.5 through a nonlinear pushover analysis curve with the estimated R factor, shown in Figure 10.

(a) Determination of R Factor by Iteration   (b) Determination of Ω0 by Pushover Curve
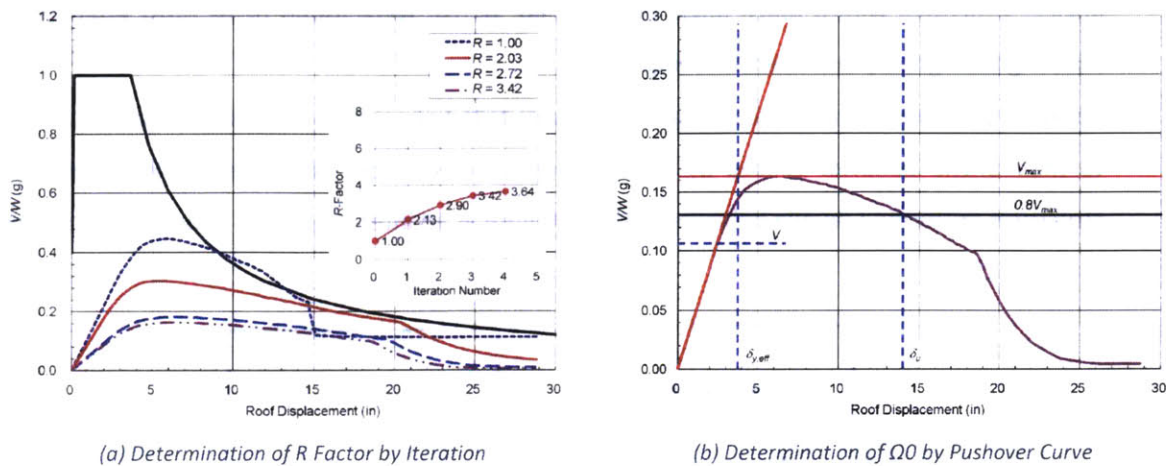
Figure 10 Determination of R and Ω₀ (Baker et al.)

4.2 Seismic Evaluation of Diagrid System by Kim and Lee

J. Kim and Y.-H. Lee presented a paper evaluating the seismic performance of Diagrid system buildings. They analyzed the seismic behavior of several 36-story buildings with varying diagonal angles from 50° to 80° in comparison with a pure tubular structure (i.e. equivalent to a brace angle of 90°). They conducted the seismic analysis according to IBC 2006, using nonlinear static pushover analysis and dynamic time-history analysis.

Key conclusions drawn from Kim and Lee's study are summarized below:

- According to their research, as the slope of the diagonals increased, the fundamental period of the building increased and the shear lag effect increased while the lateral strength of the building reduced, as shown in Figure 11.

			Fundamental mode	
Model	V_d (kN)	V_d/W	Period (s)	Modal participation mass (%)
DS-50.2	9261.8	0.178	2.67	59.2
DS-61.0	9128.2	0.188	2.59	61.9
DS-67.4	9136.1	0.187	2.69	64.1
DS-71.6	9133.3	0.187	2.87	66.1
DS-74.5	9121.2	0.188	3.14	67.2
DS-79.5	9163.7	0.185	3.82	69.6
TS	9238.7	0.179	4.90	69.1

Figure 11 Fundamental Mode Response of Varying Diagrids (Kim & Lee)

22

- As a result of the comparison study of different Diagrid structural models with varying diagonal angles, structures with a brace angle between 60° to 70° were found to be most effective in resisting both gravity and lateral loading.

- Comparing to tubular structures, Diagrid structures failed at an inter-story drift of under 1% due to their brittle behavior caused by the buckling of lower story diagonals; while the tubular structures performed ductile behavior until the failure at an inter-story drift of near 2.5%, shown in Figure 12.
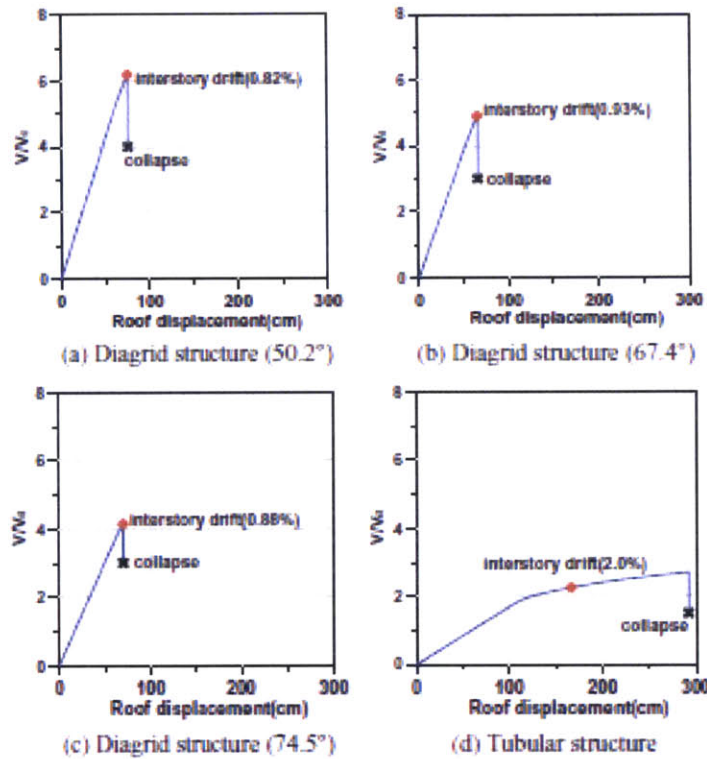
Figure 12 Pushover Curves for Diagrid Structures and Tubular Structure

- The shear lag effect of a circular Diagrid structure was found to be lower than a square Diagrid structure while Diagrids in general were experiencing less shear lag effect than tubular structures.

- Replacing the diagonals by buckling restrained braces (BRBs) would dramatically increase the strength as well as the ductility of the Diagrid structure.

Chapter 5 Model Definitions and Analysis Methodology

5.1 Model Definitions

Archetype models are critical in investigating the different behaviors of Diagrid structures because these models are the base of comparison studies. Key assumptions have to be made in order to validate the comparison procedures and their corresponding results. Identifying the proper variables in the comparison study is also of great importance. Detailed model definitions considering various prospects are presented in the following.

5.1.1 Aspect Ratio

Aspect ratio refers to the height to width ratio of a building structure. For Diagrid system, aspect ratio is one of the most important factors governing the overall behavior of the Diagrid structure. In the practicing world of building design, most of the time structural engineers are given a specific site with fixed dimension requirements on width and length while the height of the building can vary.

In order to correspond with the real world design situation, a square plan of 42 meter by 42 meter was chosen to be the fixed footprint for different models. Two varying building heights were then determined in terms of mid-rise and high-rise scenarios. A 3.6-meter story height was used for both scenarios for consistency. For the mid-rise scenario, the building model had 8 stories with a total height of 28.8 meters, resulting in an aspect ratio of 0.69. For the high-rise scenario, the building model had 60 stories with a total height of 216 meters, resulting in an aspect ratio of 5.1. Plan and elevation views of the building models are illustrated in Figure 13.
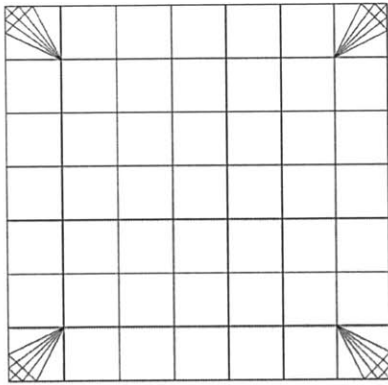
(a) Plan View of 8-story Diagrid model
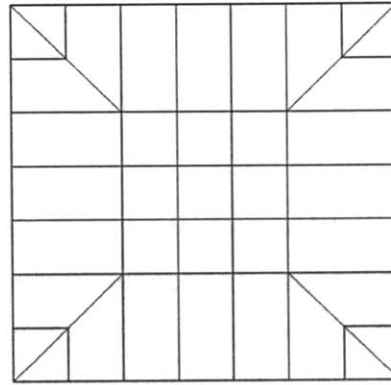
(b) Plan View of 60-story Diagrid model
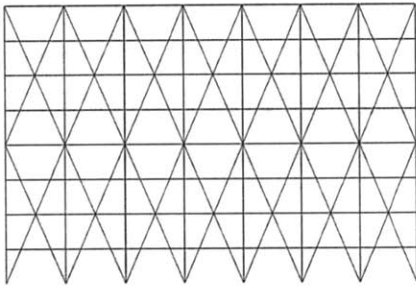
(c) Elevation View of 8-story Diagrid model
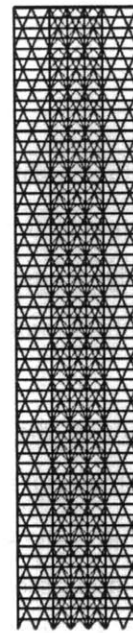
(d) Elevation View of 60-story Diagrid model
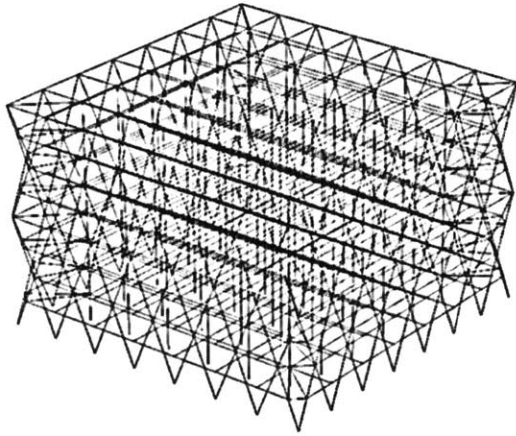
(e) 3D View of 8-story Diagrid model (d) 3D View of 60-story Diagrid model
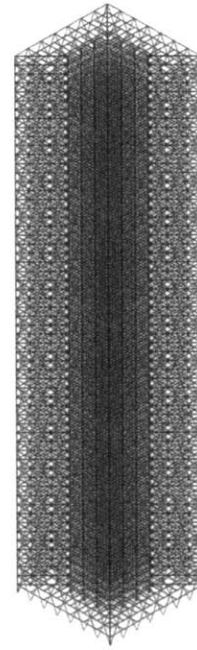
Figure 13 Plan, Elevation and 3-dimensional Views of 8-story and 60-story Diagrid Model

5.1.2 Structural Core

Ideally, for a Diagrid structure, the perimeter diagonal members can sustain both lateral and gravity loading without any additional structural support. In reality, a structural core is often incorporated with the perimeter diagonals for tall buildings, providing additional gravity and lateral stiffness to the overall structure, in order to reduce the member size of diagonals and ensure safety using a duel system.

For the two scenarios in this paper considering mid-rise and high-rise Diagrid structures, two different structural schemes were developed. For the 8-story model, no core was introduced and the Diagrid functioned as the only structural system in the design for lateral loads. For the 60-story high-rise model, a structural core was included with the perimeter diagonal members. The core was developed to be a braced frame, which is commonly used in current Diagrid core design. The braced frame core had a square plan of 18 meter by 18 meter, located in the center of the structure and connected to the perimeter Diagrids through transverse beams.

Also, for the mid-rise scenario, no corner column was included in the model while for the 60-story models, corner columns were designed as part of the Diagrid system. Illustration of these two structural schemes is shown in Figure 13 of previous section 5.1.1.

5.1.3 Diagonal Angle

Diagrid angle is another key factor in Diagrid analysis and several studies have been done in finding the optimal angle of the diagonal members. K.-S. Moon, J. J. Connor and J. E. Fernandez found out that for 60-story Diagrid buildings with an aspect ratio of around 7, the optimal diagonal angle lies between 65° to 75°. They also determined that for a building with an aspect ratio of around 5, the optimal angle range is reduced by about 10°, resulting in the range of 55° to 65°, due to the decrease in bending for a lower building (Moon et al., 2005). Similarly, as discussed in previous section 4.2, Kim and Lee investigated the behavior of several 36-story Diagrid buildings with an aspect ratio of 3.6. They concluded that the structure would become most effective when the diagonal angle was between 60° to 70° (Kim and Lee, 2010).

The primary focus of this paper was to investigate the differences in response caused by material and limit the effect of varying Diagrid angles. A single fixed diagonal angle was developed for both building heights in order to validate the comparison study between mid-rise and high-rise. Taking advantage of previous research results by Moon et al. and Kim and Lee, the diagonal angle in this research was set to be 67.4°, which is within the optimal angle range for Diagrid designs, shown in Figure 14.
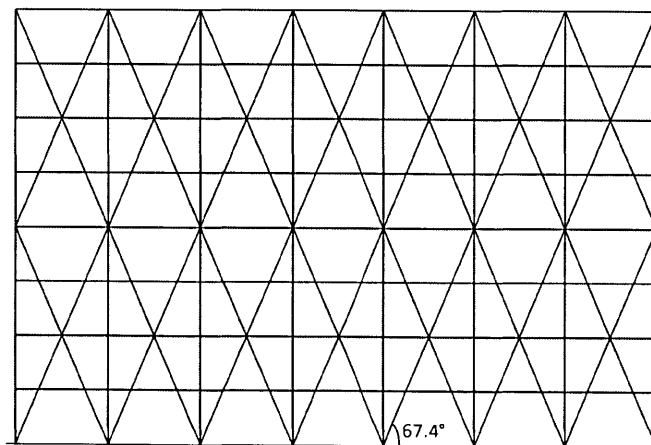
Figure 14 67.4° Angle for Diagrid Model

27

5.1.4 Material

Two materials investigated in this research were steel and prestressed concrete. For each building height scenario, two distinct models were developed composed of the two materials for comparison studies.

5.1.5 Other Structural Systems

In order to have a more thorough understanding of the Diagrid structures in the current building design environment, a comparison study between Diagrid system and other prevalent structural systems was of great value and included in this paper. For the mid-rise situation, an 8-story steel moment frame structure with the same dimension as the other Diagrid models was used for comparison study, as illustrated in Figure 15.
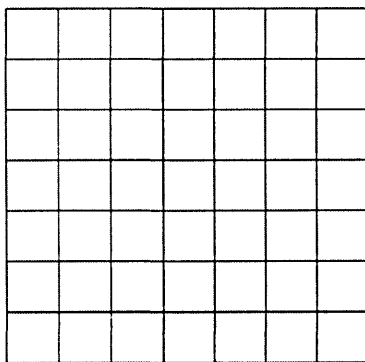
(a) Plan View of 8-story Moment Frame   *(b) Elevation View of 8-story Moment Frame*
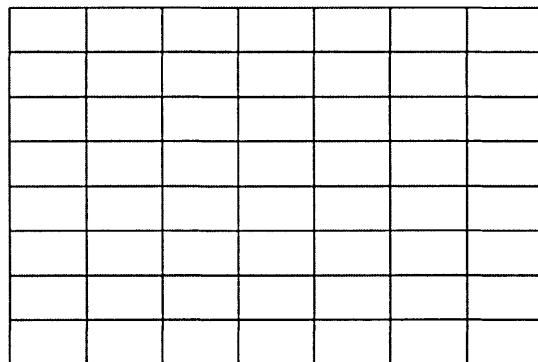
Figure 15 Plan and Elevation View of 8-story Moment Frame Model

For the high-rise 60-story building, a steel outrigger-core system structure was developed. The core was designed to be the same as the other Diagrid cores using braced frame with the same core area. Two outriggers were modeled in the structure: one at the mid-elevation (30 stories) and the other one at the top (60 stories). Plan and elevation views of this outrigger system building are shown in Figure 16.
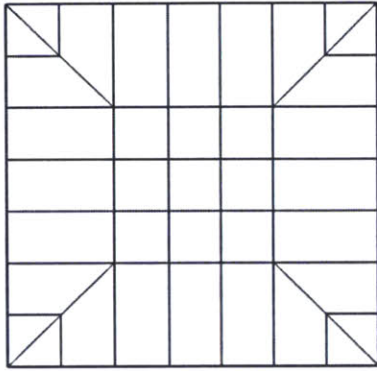
| (a) Plan View of 60-story Outrigger Model | (b) Elevation View of 60-story Outrigger Model |
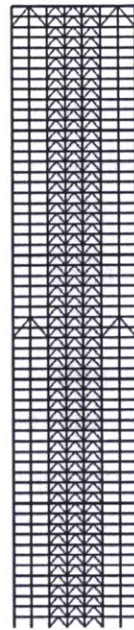
Figure 16 Plan and Elevation View of 60-story Outrigger Model

5.1.6 Building Location

For seismic evaluations, building location governs the intensity of the earthquake loading on the structure. Two different locations were considered in this paper: one in a low seismic shaking intensity area (Boston) and the other one in a high seismic shaking intensity area (San Francisco), as shown in Figure 17 from FEMA E-74 Chapter 3.3.1.
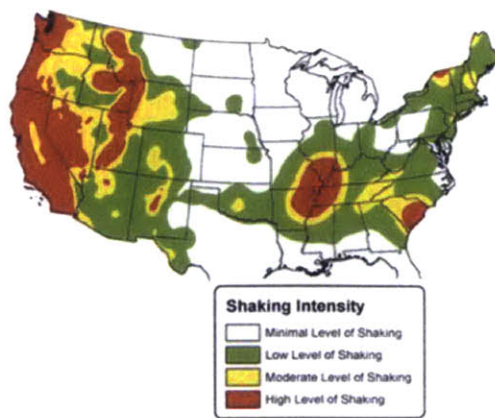
Figure 17 Seismic Shaking Intensity Map (FEMA E-74)

5.2 Analysis Methodology

The focus of this paper was to investigate and compare the seismic behavior of Diagrid structures using different materials as well as some prevalent structural systems through ASCE 7-10 code based design procedures, detailed in previous Chapter 3. An overview of the analysis methodology used for this paper is described in this section.

Model geometries were initially developed through AutoCAD and then imported into finite element software for seismic analysis. GSA was the main finite element software used in this thesis.

From the soil data provided by United States Geological Survey (USGS) shown in Figure 18, all San Francisco building models were chosen to be categorized as Site Class B. For simplicity and better comparison study, all Boston models were chosen as Site Class B as well.

Legend

—— Historic Faults

—— Holocene Faults

---- Major Roads

    Roads

    NEHRP A, B

    NEHRP C

    NEHRP D

    NEHRP E
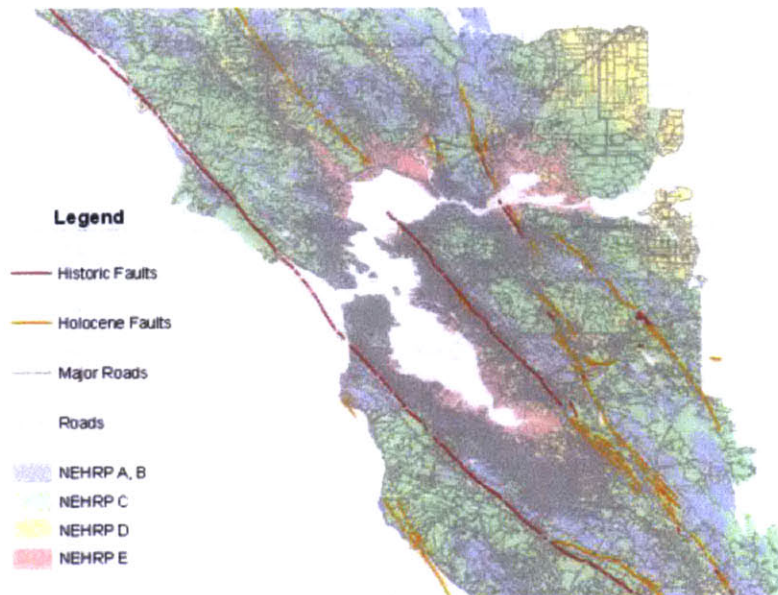
Figure 18 San Francisco Bay Area Soil Type and Shacking Hazard Map (USGS)

The design dead load was set to be 3.5 kN and the design live load was set to be 2.5 kN for all structural models. The seismic design parameters S_S, S_1 and T_L for the two locations obtained from ASCE 7-10 Chapter 22 maps are presented below in Table 1. F_a and F_v values are all 1.0 for both locations based on Site Class B condition.

Table 1 Seismic Parameters S_S, S_1 and T_L for Boston and San Francisco (ASCE 7-10)

Seismic Parameters	Boston	San Francisco
S_S	0.25	2.00
S_1	0.08	0.95
T_L	6.0 sec	12.0 sec

Member sizing of different models were then determined by setting them constant throughout different models. All models were designed to have the same member cross sections and the only difference among different models was the material difference. This criteria was utilized to maximize the effect of material by setting all the other parameters fixed throughout the analysis.

The models were then analyzed in the finite element software GSA. Response spectrum analysis was conducted to investigate the dynamic behavior of the models. For each of the two locations, a response spectrum was determined using ASCE 7-10 guidelines which was detailed in previous Chapter 3. The resulting seismic response spectrum parameters calculated for the two locations are shown in Table 2 with the corresponding equation included on the left column.

Table 2 Response Spectrum Parameters for Boston and San Francisco

Response Spectrum Parameters	Boston	San Francisco
S_S	0.25	2.00
S_1	0.08	0.95
F_a	1.0	1.0
F_v	1.0	1.0
$S_{MS} = F_a \times S_S$	0.25	2.00
$S_{M1} = F_v \times S_1$	0.08	0.95
$S_{DS} = \dfrac{2}{3} S_{MS}$	0.17	1.33
$S_{D1} = \dfrac{2}{3} S_{M1}$	0.05	0.63
$T_0 = 0.2 \times \dfrac{S_{D1}}{S_{DS}}$	0.064 sec	0.095 sec
$T_s = \dfrac{S_{D1}}{S_{DS}}$	0.32 sec	0.47 sec
T_L	6.0 sec	12.0 sec

In order to exert some real seismic excitations to the models, a number of known earthquake records were used in the analysis. Based on ASCE 7-10 requirements, three distinct earthquake data need to be considered for seismic evaluation. A total of six earthquake records were selected from PEER Ground Motion Database for the two sites including San Francisco Earthquake (1957) and Loma Prieta Earthquake (1989). The initial approach was to use linear time history analysis with the scale factor λ being applied as a base excitation to the models.

A scaled response spectrum analysis approach was alternatively used here to conduct the dynamic investigation. With the acquired ground motion data from PEER, spectral accelerations S_a were calculated and then scaled to fit the corresponding design response spectrum according to ASCE 7-10 using MatLab program. Two sets of scale factor λ were developed for the two building height scenarios in order to fit with the corresponding modal periods (Table 3 and Table 4). Figures showing design response spectrum and response spectra of earthquake records scaled for the analysis of 60-story models are presented in Figure 19 and Figure 20.
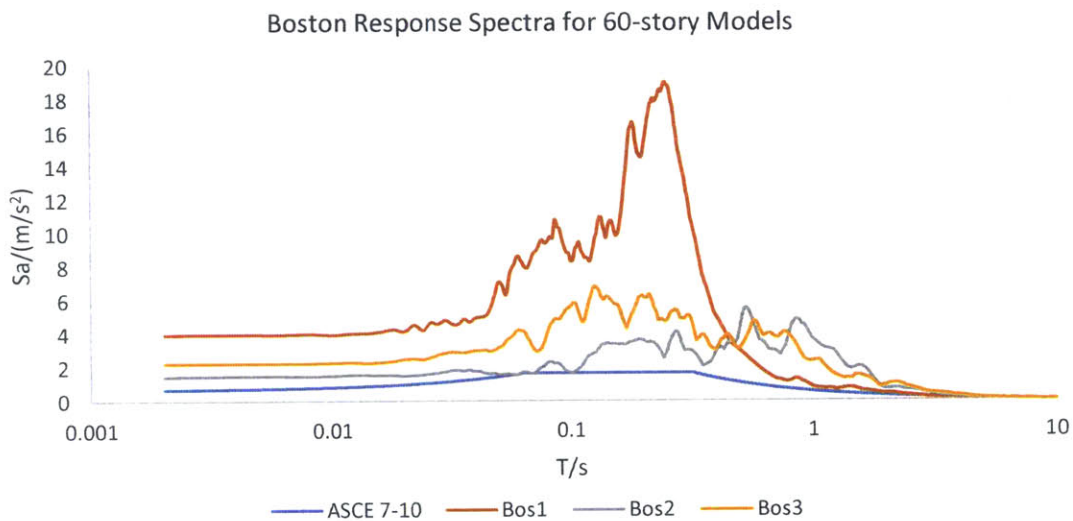
Figure 19 The Response Spectra of Selected Earthquakes in Boston for 60-story Models

San Francisco Response Spectra for 60-story Models
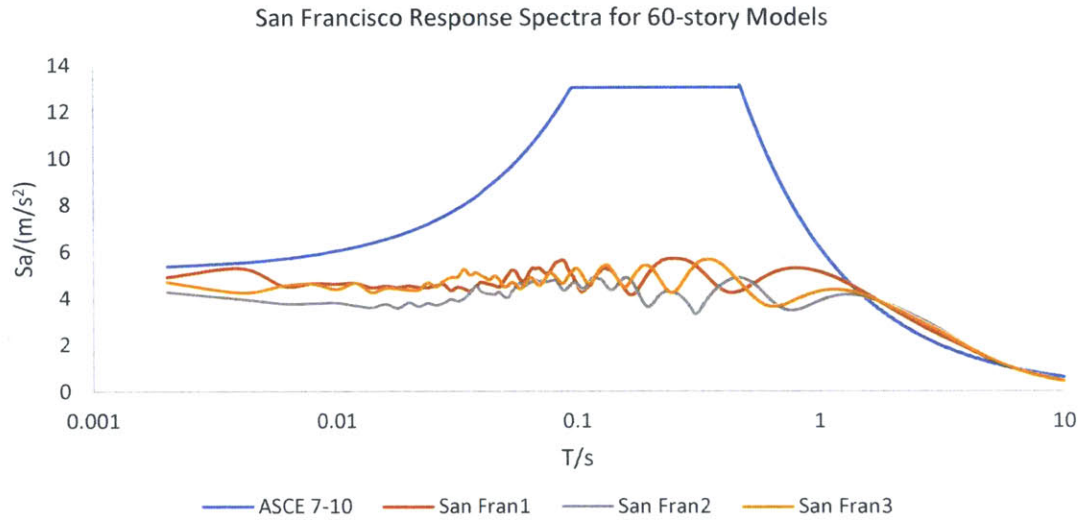
Figure 20 The Response Spectra of Selected Earthquakes in San Francisco for 60-story Models

Table 3 Response Spectrum Scale Factors for 60-story Models

	Earthquake Records					
	Bos1	Bos2	Bos3	San Fran1	San Fran2	San Fran3
scale factor λ	3.95	1.48	2.23	14.78	7.00	4.14

The scaling of the response spectra for both graphs (Figure 19 and Figure 20) were based on the fundamental periods of the three different 60-story models (steel Diagrids, concrete Diagrids and outrigger system). The process for obtaining scaled response spectra for the 60-story models is as follows and the Matlab codes implementing the process are provided in Appendix A.

- Calculate the spectral accelerations S^0_{ar} (a 5000×1 array, since it was calculated for 10sec with a time step of 0.002s) for each record r ($r = 1,2,3$).

- Obtain the fundamental periods of the three different 60-story models, which are 5.4sec, 9.4sec and 9.6sec respectively.

- Determine the spectral accelerations in ASCE spectrum ($a_m^{(ASCE)}$) and the spectrum of record 1, 2 and 3 ($a_m^{(record\ r)}$) corresponding to the fundamental period of model m ($m = 1$ refers to the steel Diagrids, $m = 2$ refers to the concrete Diagrids and $m = 3$ refers to the outrigger system).

- Calculate the scale factor λ for each record based on the criteria that the value of $\sum_m (a_m^{(ASCE)} - \lambda a_m^{(record\ r)})^2$ is the minimum.

- Multiply each element in S_{ar}^0 by λ to get the scaled spectral accelerations S_{ar} for each record r.

It could be noted that due to the scaling was based on the modal periods of 5.4sec, 9.4sec and 9.6sec, the scaled response spectra of earthquake records match the ASCE spectrum better after 5sec (the targeted range). Zoom-in views of the period range 5-10sec for the response spectra of the two locations for the analysis of 60-story models are shown in Figure 21 and Figure 22 to provide a closer look at the matched spectrums.
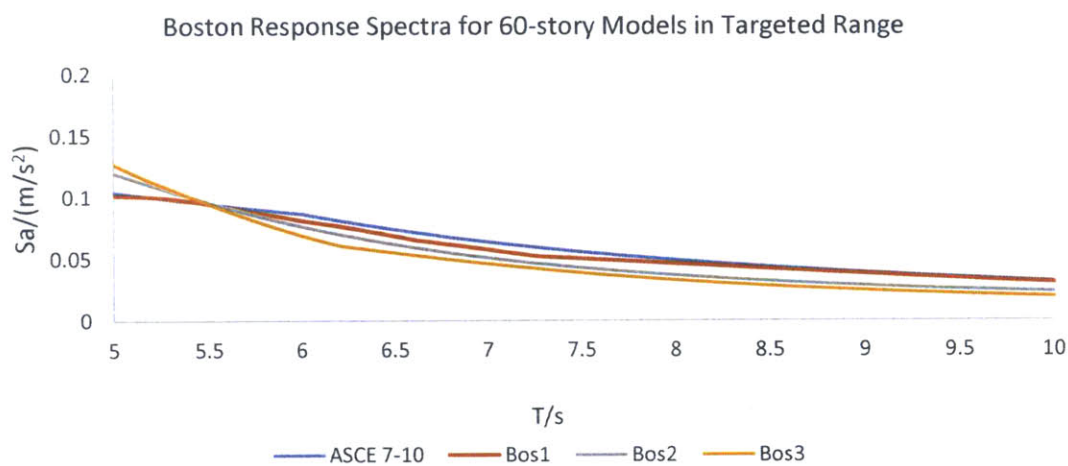
Figure 21 Zoom-in views of Response Spectra of Boston Earthquakes for 60-story Models from 1 to 6sec
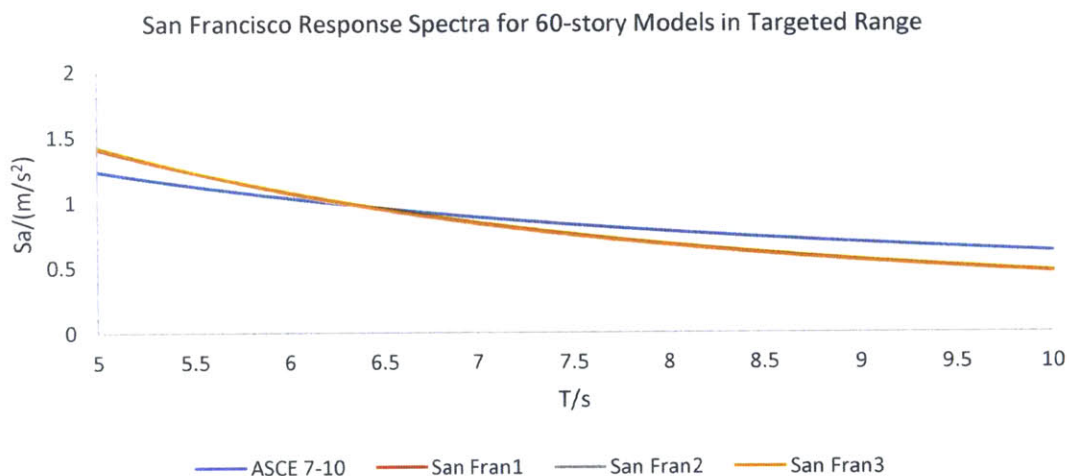
Note: the scaled spectra for the earthquake records are too close to be distinguished separately in the graph.

Figure 22 Zoom-in views of Response Spectra of San Francisco Earthquakes for 60-story Models from 1 to 6sec

The process of obtaining scaled response spectra for the 8-story models was performed in a similar way except that the values of modal periods selected were different. Thus the related spectral accelerations, scaling factors and resultant scaled spectra were different, as shown in Figure 23, Figure 24 and Table 4. Similar to the spectra for 60-story models, since fundamental periods of 0.6sec (fundamental period of the steel Diagrids), 1.4sec (fundamental period of the moment frame) and 1.5sec (fundamental period of the concrete Diagrids) were selected as the basis for scaling, the scaled spectra match the ASCE spectrum better in the targeted period range between 0.5sec and 1.5sec.

Boston Response Spectra for 8-story Models
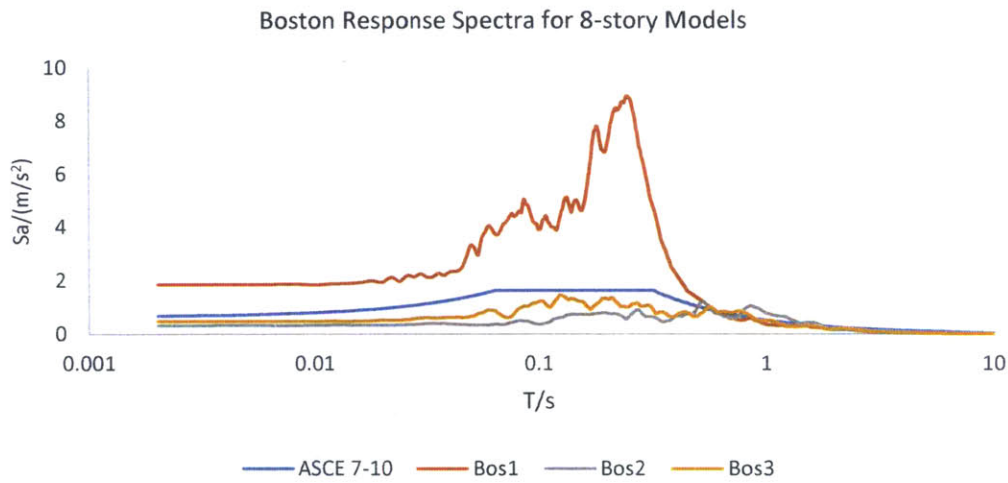
Figure 23 The Response Spectra of Selected Earthquakes in Boston for 8-story Models

San Francisco Response Spectra for 8-story Models
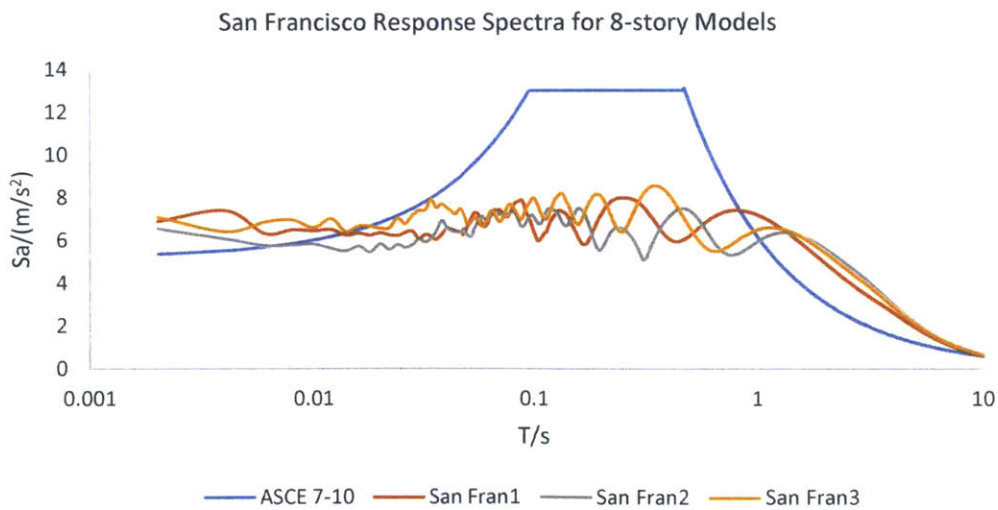
Figure 24 The Response Spectra of Selected Earthquakes in San Francisco for 8-story Models

Table 4 Response Spectrum Scale Factors for 8-story Models

	Earthquake Records					
	Bos1	Bos2	Bos3	San Fran1	San Fran2	San Fran3
scale factor λ	1.86	0.32	0.48	20.73	10.75	6.25

After the analysis process of the models, results were gathered and several comparison studies were performed on various aspects. The detailed results and comparison discussions are presented in the next several chapters with each chapter concentrating on one distinct perspective.

Chapter 6 Comparison Study of 60-Story Buildings

The first comparison study was conducted on the 60-story building models. Three structural systems were taken into consideration consisting concrete Diagrids, steel Diagrids and outrigger system. Two locations Boston and San Francisco were chosen for two seismic categories and eight different response spectra input were loaded to the buildings (for each location, there is one ASCE 7-10 based response spectrum and three earthquake record based responses spectra). As a result, a total of 24 distinct models were analyzed for comparison studies.

6.1 Modal Properties

Dynamic modal analysis was first performed on these models in order to have an overview of the mode shapes and their corresponding frequencies. The mass of the floor slabs were included in the analysis as the *Mass derived from loads* option in GSA since no slab elements were modeled in the structure. As previously stated in section 5.2, the dimension of all elements were kept as the same in order to compare the response of different models based on material differences.

6.1.1 Natural Periods

A comparison of fundamental periods of these structures provided us an initial understanding of the overall stiffness of the building under dynamic loading. Fundamental periods and their corresponding frequencies of the three models are present below in Table 5.

Table 5 Fundamental Period and Frequency for 60-story Models

System	Fundamental Period (sec)	Frequency (Hz)
Steel Diagrids	5.351	0.187
Concrete Diagrids	9.393	0.106
Outrigger System	9.605	0.104

As the analysis showed, steel Diagrids were tested to be the most stiff of all three types of structures with a fundamental period of only 5.351 seconds. For concrete Diagrid model, short term concrete was selected in GSA as the material type and a prestress force was also included considering the fact of tension

in diagonal members under lateral loads. From the analysis result, the natural period of concrete Diagrids was greater than steel Diagrids. This was mainly due to the fact that the mass of the two models were dramatically different. Given the criteria of fixing the member sizes of the models, steel structures had a bigger mass comparing to that of concrete structures due to steel's greater density. Also, modulus of elasticity of steel is approximately six times the value of high strength concrete. Considering these two factors, concrete Diagrid structures were expected to have a fundamental period of one to two times than that of steel Diagrids, which was proved in the analysis results.

When comparing to the prevalent outrigger system, concrete Diagrids had a similar fundamental period. However, both using steel and with the same member dimensions, steel Diagrid structural system was tested to be of greater stiffness than outrigger system. This finding showed that when using the same amount of steel for a 60-story building, it turned out that using a Diagrid system would be more effective in reducing fundamental period and increasing stiffness comparing to outrigger system design.

6.1.2 Mode Shapes

Other than the first modal response, a number of higher modes were also investigated during the analysis to study the mode shapes of different structures. Both concrete and steel Diagrids showed almost the same pattern of mode shapes due to their similarity in geometries and structural system. Figures showing the selected mode shapes of Diagrid system (steel Diagrid model is shown unless stated otherwise) and outrigger system are present in Figure 25.
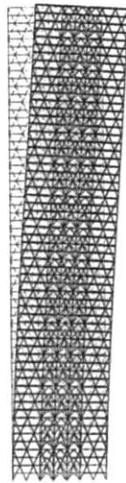
(a) Mode 1 of 60-story Diagrids   *(b) Mode 2 of 60-story Diagrids*
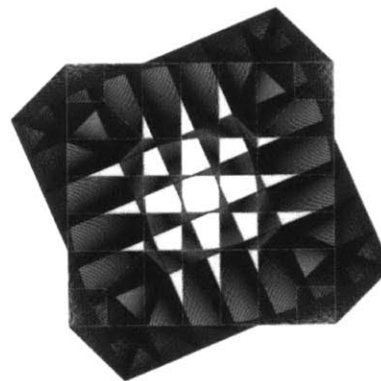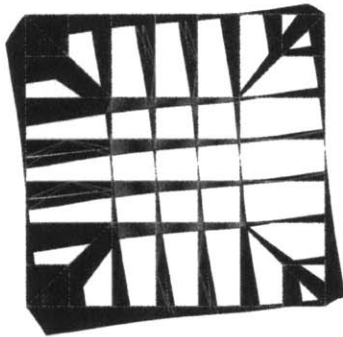
(c) Mode 1 of 60-story Outrigger System   (d) Mode 2 of 60-story Outrigger System
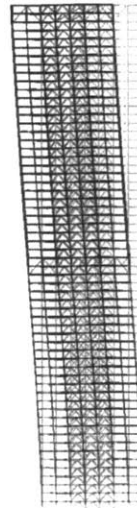
Figure 25 Selected Mode Shapes of Diagrids and Outrigger System

As the mode shapes illustrated, Diagrid structures turned out to be more susceptible to translational modes while outrigger system showed more concerns in torsional modes. For Diagrid structures, the perimeter triangulated members are functioning to confine the entire structure from torsional deformations. In addition, for a tall Diagrid building structure over 200 meters, the diagonal members work as a cantilever truss beam, for which the primary movements happen in translational directions (instead of out-of-plane torsions). On the other hand, for the outrigger system, it was mainly torsion causing the problem. This result was partly due to the fact that there were no belt trusses included for the outrigger model. Conventional outrigger systems are not able to provide much help in controlling torsional deformations while they control the lateral drifts mainly through restraining the bending of the structures.

6.2 Response Spectrum Analysis

Linear response spectrum analysis was then conducted to investigate the seismic response of the building models. The development of design and scaled response spectra were presented earlier in section 5.2. The applied design and scaled response spectra for selected earthquakes in Boston and San Francisco for 60-story building models are presented below in Figure 26 and Figure 27.

Boston Response Spectra for 60-story Models
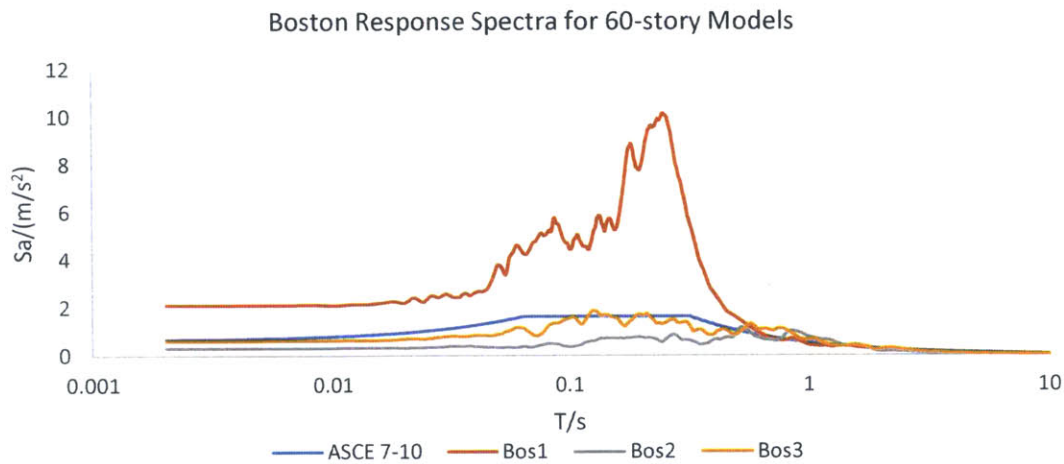
Figure 26 The Response Spectra of Selected Earthquakes in Boston for 60-story Models

San Francisco Response Spectra for 60-story Models
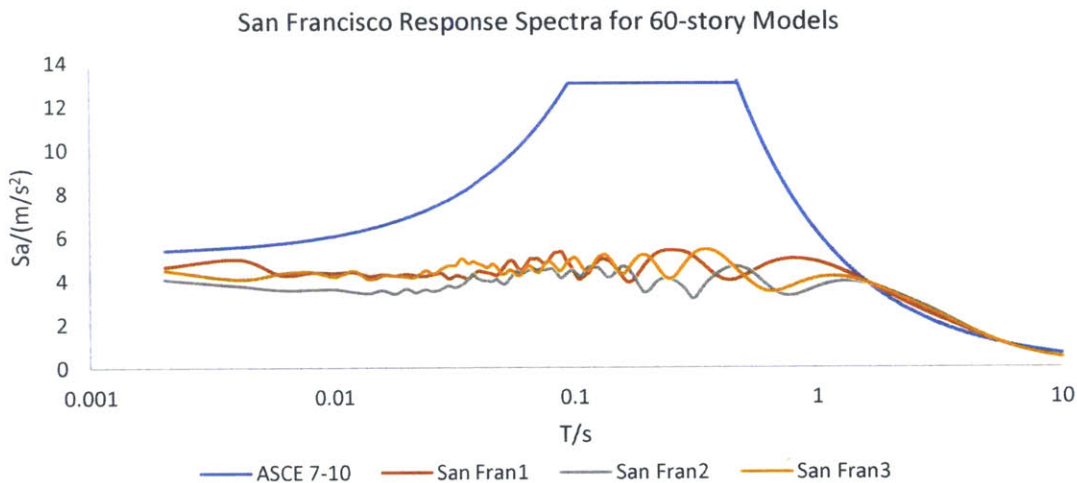
Figure 27 The Response Spectra of Selected Earthquakes in San Francisco for 60-story Models

6.2.1 Top Drift

Displacements at the top of the building structures were first investigated and compared among various models. The top drifts Δ of different 60-story models for each location are summarized in Table 5 and Table 6 respectively.

40

Table 6 Top Drifts Δ of Different 60-story Models Subjected to Boston Earthquakes

	Steel Diagrids/m	Concrete Diagrids/m	Outrigger System/m
ASCE Spectrum	0.1047	0.1193	0.1158
Bos1 Spectrum	0.1071	0.1168	0.1116
Bos2 Spectrum	0.1280	0.1096	0.0841
Bos3 Spectrum	0.1188	0.1065	0.0719

Table 7 Top Drifts Δ of Different 60-story Models Subjected to San Francisco Earthquakes

	Steel Diagrids/m	Concrete Diagrids/m	Outrigger System/m
ASCE Spectrum	1.243	2.193	2.029
San Fran1 Spectrum	1.360	1.717	1.637
San Fran2 Spectrum	1.362	1.701	1.614
San Fran3 Spectrum	1.361	1.702	1.618

Since the earthquake loading in Boston area is small, the difference between the lateral drift performances of different types of earthquakes are not obvious. However, the differences get much more significant when the models are subjected to larger earthquakes in San Francisco area. As indicated by Table 7, the top drifts for the concrete Diagrids and outrigger system for ASCE spectrum analysis are two times that of the steel Diagrids. It can be concluded that the stiffer steel Diagrids with a fundamental period of 5sec has better performance in controlling earthquake-induced lateral drifts than the more flexible concrete Diagrids and outrigger system.

6.2.2 Top Accelerations

Similar comparisons of the accelerations at the top of the structures a_t were also conducted. The results are presented in Table 8 and Table 9.

Table 8 Top Accelerations a_t of Different 60-story Models Subjected to Boston Earthquakes

	Steel Diagrids (m/s^2)	Concrete Diagrids (m/s^2)	Outrigger System (m/s^2)
ASCE Spectrum	0.2965	0.1429	0.0583
Bos1 Spectrum	0.5398	0.1710	0.0562
Bos2 Spectrum	1.3410	0.3966	0.0424
Bos3 Spectrum	0.9221	0.4501	0.0362

Table 9 Top Accelerations a_t of Different 60-story Models Subjected to San Francisco Earthquakes

	Steel Diagrids (m/s^2)	Concrete Diagrids (m/s^2)	Outrigger System (m/s^2)
ASCE Spectrum	3.5210	1.8540	1.0220
San Fran1 Spectrum	3.6360	2.0280	0.8243
San Fran2 Spectrum	3.4420	2.1740	0.8131
San Fran3 Spectrum	3.5170	2.1140	0.8149

It is noticed that the outrigger system in general has better performance in controlling earthquake-induced accelerations than the Diagrids. For the Diagrids, the concrete structures have smaller accelerations than the steel Diagrids. As for the different structural systems, the outrigger system behaves in a bending way, for which bending deformation dominates; the Diagrid system behaves in a translational way, for which transverse motions dominates. The different behaviors of the two structural systems are the fundamental reason why outrigger system is more effective in controlling accelerations.

As for the different materials used in the Diagrids, since concrete Diagrid model has larger natural periods than the steel model, the corresponding spectral accelerations of the concrete model are lower. This explains why the combined acceleration results for the first five modes of the concrete model are smaller than those of the steel model.

Chapter 7 Comparison Study of 8-Story Buildings

Similar comparison study to that of 60-story building models were performed to analyze the 8-story models. Three structural systems were taken into consideration including a concrete Diagrids, steel Diagrids and moment frame. The locations considered and response spectra loaded were the same as presented in Chapter 6.

The GSA analysis settings and assumptions for the 8-story buildings were the same as those in the 60-story models illustrated in Chapter 6, and they are not repeated in this chapter. The analysis results are presented in the following sections for discussions.

7.1 Modal Properties

7.1.1 Natural Periods

The fundamental periods and frequencies of the three different 8-story models are summarized in Table 10.

Table 10 Fundamental Period and Frequency for 8-story Models

System	Fundamental Period (sec)	Frequency (Hz)
Steel Diagrids	1.485	0.674
Concrete Diagrids	3.920	0.255
Moment Frame	3.588	0.279

Similar comparison results were obtained as those in section 6.1.1. The steel Diagrids is still the most stiff among the three. Due to the much decreased height, the stiffness of the moment frame gets larger, which even exceeds that of the concrete Diagrids in the situation.

7.1.2 Mode Shapes

Mode shapes of the three 8-story building models were also investigated. Figures showing the selected mode shapes of Diagrid system (steel Diagrid model is shown unless stated otherwise) and moment frame system are present in Figure 28.

(a) Mode 1 of 8-story Diagrids

(b) Mode 2 of 8-story Diagrids

(c) Mode 3 of 8-story Diagrids

(d) Mode 1 of 8-story Moment Frame

(e) Mode 2 of 8-story Moment Frame

(f) Mode 3 of 8-story Moment Frame
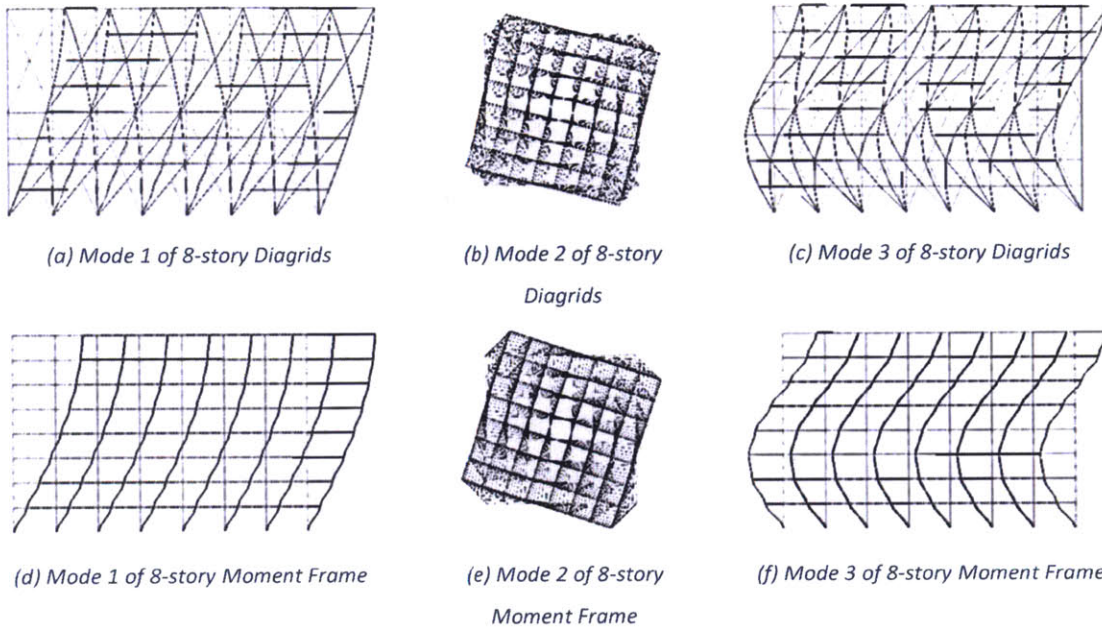
Figure 28 Selected Mode Shapes of Diagrids and Moment Frame

As the figures illustrated, all three structures had almost the same mode shapes with the first mode being translational, second being torsional and the others also translational. This result showed that for a mid-rise 8-story building, both Diagrid structures and moment frame structures are more concerned with lateral modes instead of torsional modes.

7.2 Response Spectrum Analysis

The spectra used in the analysis were shown in Figure 29(Boston) and Figure 30(San Francisco), which were scaled according to the process clarified in section 5.2.

Boston Response Spectra for 8-story Models
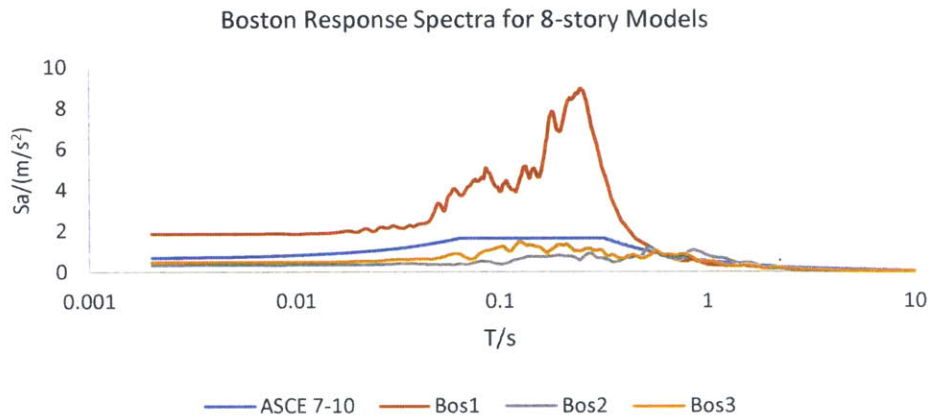
Figure 29 The Response Spectra of Selected Earthquakes in Boston for 8-story Models

San Francisco Response Spectra for 8-story Models
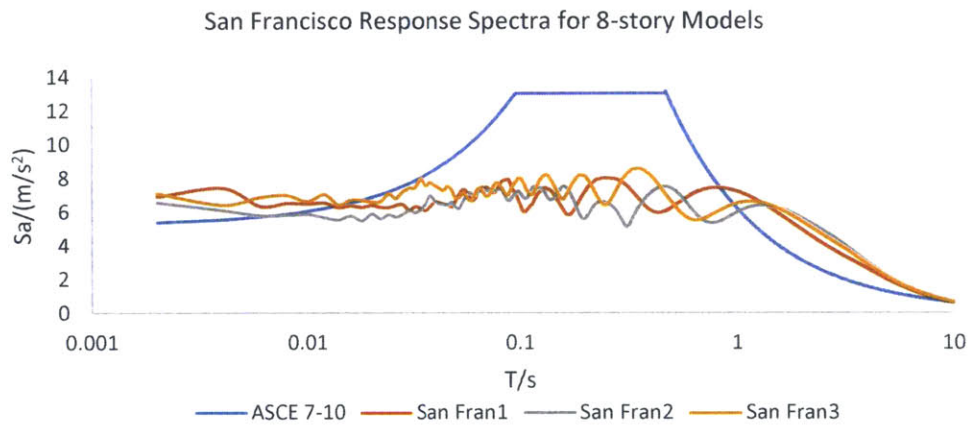
Figure 30 The Response Spectra of Selected Earthquakes in San Francisco for 8-story Models

7.2.1 Top Drift

The top drifts Δ of different 8-story models for two locations are summarized in Table 11 and Table 12.

Table 11 Top Drifts Δ of Different 8-story Models Subjected to Boston Earthquakes

	Steel Diagrids/m	Concrete Diagrids/m	Moment Frame/m
ASCE Spectrum	0.0251	0.0658	0.0605
Bos1 Spectrum	0.0235	0.0260	0.0272
Bos2 Spectrum	0.0299	0.0194	0.0215
Bos3 Spectrum	0.0224	0.0292	0.0311

Table 12 Top Drifts Δ of Different 8-story Models Subjected to San Francisco Earthquakes

	Steel Diagrids/m	Concrete Diagrids/m	Moment Frame/m
ASCE Spectrum	0.2978	0.7818	0.7182
San Fran1 Spectrum	0.4297	1.3370	1.2350
San Fran2 Spectrum	0.4450	1.5220	1.4290
San Fran3 Spectrum	0.4475	1.4800	1.3830

Similar to what happened to the 60-story models, the steel Diagrids is the most stiff, which has the minimum top drift among the three. In general, the Diagrid structural system is better in controlling top drift than the moment frame.

7.2.2 Top Accelerations

Similar comparisons of the accelerations at the top of the structures a_t were also conducted. The results are presented in Table 13 and Table 14.

Table 13 Top Accelerations a_t of Different 8-story Models Subjected to Boston Earthquakes

	Steel Diagrids (m/s^2)	Concrete Diagrids (m/s^2)	Moment Frame (m/s^2)
ASCE Spectrum	0.6133	0.1691	0.2526
Bos1 Spectrum	0.6896	0.0667	0.1495
Bos2 Spectrum	0.6674	0.0499	0.2650
Bos3 Spectrum	0.4862	0.0749	0.1633

Table 14 Top Accelerations a_t of Different 8-story Models Subjected to San Francisco Earthquakes

	Steel Diagrids (m/s^2)	Concrete Diagrids (m/s^2)	Moment Frame (m/s^2)
ASCE Spectrum	7.2830	2.0080	2.9990
San Fran1 Spectrum	8.0950	3.4350	4.6390
San Fran2 Spectrum	8.4980	3.9100	5.0490
San Fran3 Spectrum	8.4380	3.8030	4.9870

It is shown that steel Diagrids is much less satisfying in controlling the accelerations compared with concrete Diagrids and moment frame, same as the results for 60-story models. However, although for 60-story models, the outrigger system has smaller accelerations than both steel and concrete Diagrids, this time the moment frame is worse in controlling accelerations than the concrete Diagrids. This is mainly due to the increased difference in the natural periods of the concrete Diagrids and moment frame. In the 60-stody models, the concrete Diagrids and the outrigger system have very close natural periods (with a difference of 0.2sec (2%) in terms of the fundamental period). The accelerations in this case primarily rely on the structural systems. The moment deformation controlled outrigger has better performance than the translational deformation controlled concrete Diagrids.

However, for the 8-story concrete Diagrids and moment frame, the difference of natural periods gets larger and non-negligible (with a difference of 0.4sec (10%) in terms of the fundamental period). In this situation, the accelerations are not only controlled by the structural systems, but also the natural periods. Although the moment deformation controlled moment frame tends to behave better in controlling the accelerations, its larger stiffness makes it more susceptible to them at the same time.

Chapter 8 Conclusion

From the comparison study, Diagrid system showed its structural efficiency comparing to both outrigger system and moment frame system as expected. Concrete and steel Diagrid structures also showed their differences in dynamic and seismic behaviors.

The modal analysis showed that for both building height scenarios, steel Diagrids were found to be the most stiff due to its bigger mass comparing to concrete Diagrids and its greater structural system effectiveness comparing to the other two structural systems. As for the mode shapes, for the high-rise scenario, Diagrid buildings were tested to be more susceptible to translational modes while outrigger model was governed more by torsional modes. For the mid-rise scenario, all models had similar mode shapes with translational being the fundamental mode and torsional the second.

The response spectrum analysis compared the top drift and top acceleration of the models under the design ASCE spectrum and scaled earthquake spectra. Steel Diagrids were tested to be the most stiff while Diagrid structural system was better in controlling top drift than moment frame and outrigger systems. From the top acceleration perspective, concrete Diagrid models had lower top acceleration comparing to steel Diagrids because concrete Diagrids has larger natural periods. However, Diagrid systems performed less satisfying in controlling top accelerations than the other two systems due to the different behaviors of the two system, for which outrigger and moment frame behave in a bending way and Diagrid system behaves in a translational way.

For fixed member sizes and dimension, steel Diagrids behave relatively better than concrete Diagrids under seismic events while Diagrid system shows its effectiveness in restraining top drifts but lack of limitation on top accelerations. With limited amount of information on the seismic behavior of Diagrid structures, further research should be taken considering from other criteria such as limit the top drift of the models to a specific value and compare the material costs of different Diagrid structures. Also, more materials could be investigated including concrete/steel composite and timber. Performance based seismic design could also be utilized to generate a more complete portfolio of seismic performance in the damage and repair aspect. As a structurally efficient and architecturally elegant system, Diagrid structural system has the potential of becoming the most dominating scheme in the future building design environment.

References

American Society of Civil Engineers (Ed.). (2010). *Minimum design loads for buildings and other structures*. Reston, Va: American Society of Civil Engineers : Structural Engineering Institute.

Baker, W., Besjak, C., Sarkisian, M., Lee, P., & Doo, C. S. (2010). Proposed methodology to determine seismic performance factors for steel diagrid framed systems. Council of Tall Buildings and Urban Habitat.

Boake, T. M. (2013). Diagrids, the New Stability System: Combining Architecture with Engineering. In *AEI 2013@ Building Solutions for Architectural Engineering* (pp. 574–583). ASCE. Retrieved from http://ascelibrary.org/doi/pdf/10.1061/9780784412909.056

Federal Emergency Management Agency, (2011). *Reducing the risks of nonstructural earthquake damage – a practical guide* (E-74)

Huang, C., Han, X., Ji, J., & Tang, J. (2010). Behavior of concrete-filled steel tubular planar intersecting connections under axial compression, Part 1: Experimental study. *Engineering Structures*, *32*(1), 60–68. http://doi.org/10.1016/j.engstruct.2009.08.016

Kim, J., & Lee, Y.-H. (2012). Seismic performance evaluation of diagrid system buildings. *The Structural Design of Tall and Special Buildings*, *21*(10), 736–749.

Liptack, R. J. (2013). Motion Based Seismic Design and Loss Estimation of Diagrid Structures. Massachusetts Institute of Technology. Retrieved from http://hdl.handle.net/1721.1/82818

Maqhareh, M. R. (2014). The Evolutionary Process of Diagrid Structure towards Architectural, Structural and Sustainability Concepts: Reviewing Case Studies. *Journal of Architectural Engineering Technology*, *03*(02). http://doi.org/10.4172/2168-9717.1000121

Moon, K.-S., Connor, J. J., & Fernandez, J. E. (2007). Diagrid structural systems for tall buildings: characteristics and methodology for preliminary design. *The Structural Design of Tall and Special Buildings*, *16*(2), 205–230. http://doi.org/10.1002/tal.311

PEER, Pacific Earthquake Engineering Research Center, "PEER Ground Motion Database". Retrieved from http://peer.berkeley.edu/products/strong_ground_motion_db.html

Singh, R. K., Garg, V. & Sharma, A. (2014) *Analysis of concrete diagrid building and its comparison with conventional frame building*. International Journal of Science, Engineering and Technology, *2*(6), 1330-1337.

U.S. Geological Survey. (2015) *Soil type and shaking hazard in the San Francisco Bay area*. Retrieved from http://earthquake.usgs.gov/regional/nca/soiltype/map/

Appendix A Matlab Codes for Obtaining Response Spectrums

```matlab
%Script One: Boston 60-Story Models

clear all
dt = 0.01;
xi = 0.05;
SD_1 = 0.52;
SD_s = 1.63;
T0 = 0.064;
Ts = 0.32;
Tl = 6;
i=1;

%periods selected as scaling basis
T_3 = 9.6;
T_2 = 9.4;
T_1 = 5.36;

%Loop for drawing the code-based response spectrum
for T = 0.002:0.002:10,
    if T < T0,
        Sa(i,1) = SD_s*(0.4+0.6*T/T0);
    end
    if (T >= T0 && T <= Ts),
        Sa(i,1)=  SD_s;
    end
    if (T > Ts && T <= Tl),
        Sa(i,1) = SD_1/T;
    end
    if T > Tl,
        Sa(i,1) = SD_1*Tl/T^2;
    end
    X (i,1)=T;
    i=i+1;
end


%Earthquake 1
data1 = importdata('record1.csv');
data1 = data1(:,2)';

%Loop for finding the scale factor
p = 1;
for x = 0:0.01:5,
for j = 1:5000,
    T1(j,1) = 0.002*j;
    Sa1(j,1)= spectralAccel(data1, dt, T1(j,1), xi);
    if T1(j,1) == T_1,
        sum_1 = (x*Sa1(j,1)-Sa(j,1))^2;
    end
    if T1(j,1) == T_2,
        sum_2 = (x*Sa1 (j,1)-Sa(j,1))^2;
```

```
        end
    if T1(j,1) == T_3,
        sum_3 = (x*Sa1 (j,1)-Sa(j,1))^2;
    end

end
sum (p,1) = sum_1+sum_2+sum_3;

if p == 1,
    sum_min = sum (p,1);
else
    if sum (p,1) < sum ((p-1),1),
        sum_min = sum (p,1);
        lamda_1 = x;
    end
end
p = p+1;
end

%Obtain scaled spectral accelerations
Sa1_new = lamda_1*Sa1;

data2 = importdata('record2.csv');
data2 = data2(:,2)';

p = 1;
for x = 0:0.01:5,
for m = 1:5000,
    T2(m,1) = 0.002*m;
    Sa2(m,1)= spectralAccel(data2, dt, T2(m,1), xi);
    if T1(m,1) == T_1,
        sum_1 = (x*Sa2(m,1)-Sa(m,1))^2;
    end
    if T1(m,1) == T_2,
        sum_2 = (x*Sa2 (m,1)-Sa(m,1))^2;
    end
    if T1(m,1) == T_3,
        sum_3 = (x*Sa2 (m,1)-Sa(m,1))^2;
    end

end
sum (p,1) = sum_1+sum_2+sum_3;

if p == 1,
    sum_min = sum (p,1);
else
    if sum (p,1) < sum ((p-1),1),
        sum_min = sum (p,1);
        lamda_2 = x;
    end
end
p = p+1;
end

Sa2_new = lamda_2*Sa2;
```

```
%Earthquake 3
data3 = importdata('record3.csv');
data3 = data3(:,2)';

p = 1;
for x = 0:0.01:10,
for n = 1:5000,
    T3(n,1) = 0.002*n;
    Sa3(n,1)= spectralAccel(data3, dt, T3(n,1), xi);
    if T3(n,1) == T_1,
        sum_1 = (x*Sa3(n,1)-Sa(n,1))^2;
    end
    if T3(n,1) == T_2,
        sum_2 = (x*Sa3 (n,1)-Sa(n,1))^2;
    end
    if T3(n,1) == T_3,
        sum_3 = (x*Sa3 (n,1)-Sa(n,1))^2;
    end

end
sum (p,1) = sum_1+sum_2+sum_3;

if p == 1,
    sum_min = sum (p,1);
else
    if sum (p,1) < sum ((p-1),1),
        sum_min = sum (p,1);
        lamda_3 = x;
    end
end
p = p+1;
end

Sa3_new = lamda_3*Sa3;

%%%%%%%%%%%%%%%%%%%%%%%%%%%%%%%%%%%%%%%%%%%%%%%%%%%%%%%%%

%Script two: San Francisco 60-story Models

dt = 0.01;
xi = 0.05;
SD_1 = 6.174;
SD_s = 13.034;
T0 = 0.095;
Ts = 0.47;
Tl = 12;
i=1;

T_3 = 9.6;
T_2 = 9.4;
T_1 = 5.36;
```

```matlab
for T = 0.002:0.002:10,
    if T < T0,
        Sa_new(i,1) = SD_s*(0.4+0.6*T/T0);
    end
    if (T >= T0 && T <= Ts),
        Sa_new(i,1)=  SD_s;
    end
    if (T > Ts && T <= Tl),
        Sa_new(i,1) = SD_1/T;
    end
    if T > Tl,
        Sa_new(i,1) = SD_1*Tl/T^2;
    end
    X (i,1)=T;
    i=i+1;
end

%Earthquake 1
data4 = importdata('SF1.csv');
data4 = data4(:,2)';


p = 1;
for x = 0:0.01:10,
for j = 1:5000,
    T4(j,1) = 0.002*j;
    Sa4(j,1)= spectralAccel(data4, dt, T4(j,1), xi);
    if T4(j,1) == T_1,
        sum_1 = (x*Sa4(j,1)-Sa_new(j,1))^2;
    end
    if T4(j,1) == T_2,
        sum_2 = (x*Sa4 (j,1)-Sa_new(j,1))^2;
    end
    if T4(j,1) == T_3,

        sum_3 = (x*Sa4 (j,1)-Sa_new(j,1))^2;
    end
end
sum (p,1) = sum_1+sum_2+sum_3;

if p == 1,
    sum_min = sum (p,1);
else
    if sum (p,1) < sum ((p-1),1),
        sum_min = sum (p,1);
        lamda_4 = x;
    end
end
p = p+1;
end

Sa4_new = lamda_4*Sa4;
```

```matlab
%Earthquake 2
data5 = importdata('SF2.csv');
data5 = data5(:,2)';

p = 1;
for x = 0:0.01:10,
for m = 1:5000,
    T5(m,1) = 0.002*m;
    Sa5(m,1)= spectralAccel(data5, dt, T5(m,1), xi);
    if T5(m,1) == T_1,
        sum_1 = (x*Sa5(m,1)-Sa_new(m,1))^2;
    end
    if T5(m,1) == T_2,
        sum_2 = (x*Sa5(m,1)-Sa_new(m,1))^2;
    end
    if T5(m,1) == T_3,
        sum_3 = (x*Sa5(m,1)-Sa_new(m,1))^2;
    end
end
sum (p,1) = sum_1+sum_2+sum_3;

if p == 1,
    sum_min = sum (p,1);
else
    if sum (p,1) < sum ((p-1),1),
        sum_min = sum (p,1);
        lamda_5 = x;
    end
end
p = p+1;
end

Sa5_new = lamda_5*Sa5;

%Earthquake 3
data6 = importdata('SF3.csv');
data6 = data6(:,2)';

p = 1;
for x = 0:0.01:5,
for n = 1:5000,
    T6(n,1) = 0.002*n;
    Sa6(n,1)= spectralAccel(data6, dt, T6(n,1), xi);
    if T6(n,1) == T_1,
        sum_1 = (x*Sa6(n,1)-Sa_new(n,1))^2;
    end
    if T6(n,1) == T_2,
        sum_2 = (x*Sa6 (n,1)-Sa_new(n,1))^2;
    end
    if T6(n,1) == T_3,
        sum_3 = (x*Sa6 (n,1)-Sa_new(n,1))^2;
    end
end
sum (p,1) = sum_1+sum_2+sum_3;
```

```
if p == 1,
    sum_min = sum (p,1);
else
    if sum (p,1) < sum ((p-1),1),
        sum_min = sum (p,1);
        lamda_6 = x;
    end
end
p = p+1;
end

Sa6_new = lamda_6*Sa6;
```